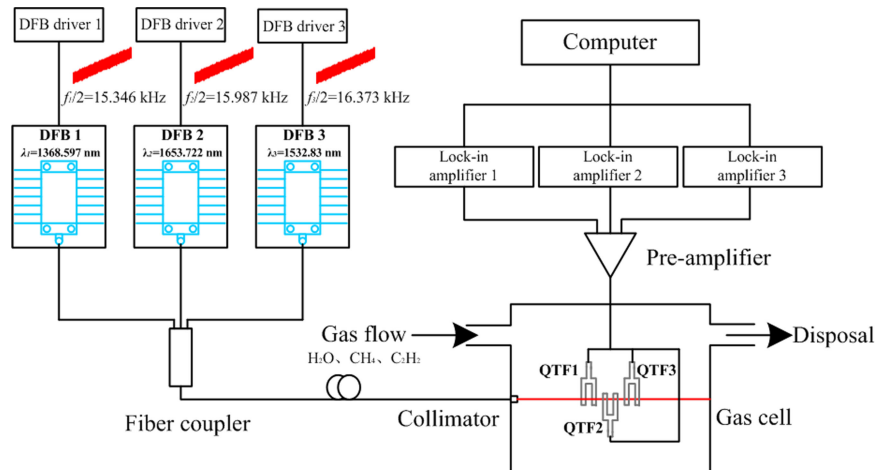


# QEPAS Sensor for Simultaneous Measurements of H<sub>2</sub>O, CH<sub>4</sub>, and C<sub>2</sub>H<sub>2</sub> Using Different QTFs

Volume 10, Number 6, December 2018

Qinduan Zhang  
Jun Chang  
Zhenhua Cong  
Jiachen Sun  
Zongliang Wang



Configuration of the multi-gas QEPAS sensor based on three different QTFs

# QEPAS Sensor for Simultaneous Measurements of H<sub>2</sub>O, CH<sub>4</sub>, and C<sub>2</sub>H<sub>2</sub> Using Different QTFs

Qinduan Zhang ,<sup>1</sup> Jun Chang ,<sup>1</sup> Zhenhua Cong,<sup>1</sup> Jiachen Sun ,<sup>1</sup> and Zongliang Wang<sup>2</sup>

<sup>1</sup>School of Information Science and Engineering and Shandong Provincial Key Laboratory of Laser Technology and Application, Shandong University, Jinan 250100, China

<sup>2</sup>School of Physics Science and Information Technology and Shandong Key Laboratory of Optical Communication Science and Technology, Liaocheng University, Liaocheng 252059, China

DOI:10.1109/JPHOT.2018.2880187

1943-0655 © 2017 IEEE. Translations and content mining are permitted for academic research only.  
Personal use is also permitted, but republication/redistribution requires IEEE permission.  
See [http://www.ieee.org/publications\\_standards/publications/rights/index.html](http://www.ieee.org/publications_standards/publications/rights/index.html) for more information.

Manuscript received August 20, 2018; revised November 1, 2018; accepted November 5, 2018. Date of publication November 9, 2018; date of current version November 22, 2018. This work was supported by National Natural Science Foundation of China under Grants 61405105 and 61475085. Corresponding author: Jun Chang (e-mail: changjun@sdu.edu.cn).

**Abstract:** A multi-gas quartz enhanced photoacoustic spectroscopy (QEPAS) sensor based on three quartz tuning forks (QTFs) with different response frequencies for trace gas detection was proposed and experimentally demonstrated. Three near-infrared DFB lasers are used to monitor water vapor, methane, and acetylene in the parts per million range. The sensor system was first evaluated for individual H<sub>2</sub>O, CH<sub>4</sub>, and C<sub>2</sub>H<sub>2</sub> detection, respectively. Subsequently, the sensor system was evaluated for simultaneous H<sub>2</sub>O, CH<sub>4</sub>, and C<sub>2</sub>H<sub>2</sub> detection. Finally, trace gas measurements have been assessed and minimum detection limit (MDL) of 1.3 ppmv at 1368.597 nm for H<sub>2</sub>O, 79 ppmv at 1653.722 nm for CH<sub>4</sub>, and 5 ppmv at 1532.83 nm for C<sub>2</sub>H<sub>2</sub> have been demonstrated. The continuous monitoring of H<sub>2</sub>O, CH<sub>4</sub>, and C<sub>2</sub>H<sub>2</sub> concentration levels for >3 h indicated the stability of the reported multi-gas QEPAS sensor system.

**Index Terms:** Gas detection, multi-component, QEPAS sensor.

## 1. Introduction

Multi-Gas sensing is playing a more and more important role in the field of pollution monitoring [1], industrial process control [2], and environmental monitoring [3], [4]. Fast time response, selective and ultra-sensitive multi-gas sensors are required for a wide array of applications. Photoacoustic spectroscopy (PAS) [5] is an effective gas sensor technology which employs a sensitive microphone for acoustic wave detection without the need of photodetectors, which allows for various types of laser sources from ultraviolet to terahertz. However, most photoacoustic cells have a low resonant frequency, which makes the photoacoustic cells more sensitive to environmental noise and gas flow noise [6]. Moreover, the size of the photoacoustic cell is also large and heavy [7]. The quartz-enhanced photoacoustic spectroscopy (QEPAS) technique was first reported in 2002 by Kosterev *et al.* [8]. This technique uses a commercial piezoelectric quartz tuning fork (QTF) as an acoustic wave transducer which possesses a high detection sensitivity and immunity to ambient acoustic noise [9].

TABLE 1  
Research Comparison

Research team	Probed gases	MDL	Technique
Ren et al.	CH <sub>4</sub>	5.9 ppbv	TDLAS
	N <sub>2</sub> O	2.6 ppbv	
Besson et al.	CH <sub>4</sub>	0.5 ppmv	PAS
	HCl	3 ppmv	
	H <sub>2</sub> O	0.2 ppmv(sensitivity)	
Wu et al.	H <sub>2</sub> O	\	QEPAS
	C <sub>2</sub> H <sub>2</sub>	\	
Kosterev et al.	H <sub>2</sub> S	ppmv level	QEPAS
	CO <sub>2</sub>	100% level	
	CH <sub>4</sub>	100% level	
Our research	H <sub>2</sub> O	1.3 ppmv	QEPAS
	CH <sub>4</sub>	79 ppmv	
	C <sub>2</sub> H <sub>2</sub>	5 ppmv	

As a promising means for trace gas detection, QEPAS sensors have attracted considerable attention in recent years because of its high sensitivity and fast time response. Dong *et al.* [10] reported a QEPAS sensor for nitric oxide detection with an external cavity quantum cascade laser, and a sensitivity of 4.9 ppbv was achieved. Petersen *et al.* [11] presented an innovative and novel QEPAS sensor for highly sensitive and selective breath gas analysis. They achieved a detection limit of 32 ppbv at 190 s integration time for methane detection. Recently, Shi *et al.* [12] employed a compact and sensitive mid-infrared NO sensor using off-beam QEPAS, and the detection limit of NO is achieved to be 120 ppbv at the wavelength of 5.2  $\mu$ m. Ma *et al.* [13] demonstrated an ultra-high sensitive QEPAS based ammonia (NH<sub>3</sub>) sensor using a power amplified diode laser and a low resonance frequency QTF. The MDL of 418.4 ppbv was achieved at a NH<sub>3</sub> absorption line of 1530.6 nm.

In the past, some QEPAS sensors used two QTFs to detect acoustic wave signal generated by laser absorption. Ma *et al.* [14] reported an M-QEPAS sensor. In this sensor, the acoustic signal was detected by two QTFs simultaneously. Compared with the traditional single QTF, the sensor resulted in a 1.7 times signal enhancement. Zheng *et al.* [15] proposed a multi-QTF based spectrophone with “on-beam” AmR configuration. This configuration had a signal enhancement of 1.6 times as compared to the sensor with one QTF. In addition, other QEPAS sensors with two QTFs have been reported in [16].

Previously, many multi-gas sensors were reported. In 2014, Ren *et al.* [17] proposed a quantum cascade laser-based absorption sensor for the simultaneous dual-species monitoring of CH<sub>4</sub> and N<sub>2</sub>O using a novel compact multipass gas cell. Besson *et al.* [18] introduced a multi-hydrogenated compounds detection system based on a PA cell and three DFB lasers to monitor methane, water vapour and hydrogen, and detection limits of 0.5 ppmv of CH<sub>4</sub>, 0.2 ppmv of H<sub>2</sub>O and 3 ppmv of HCl has been achieved. Wu *et al.* [19] described a dual-gas QEPAS sensor based on a custom-designed QTF combined excitation of the fundamental and 1st over-tone flexural modes. Kosterev *et al.* [20] developed a gas sensor based on QEPAS and using near-infrared, fiber-coupled diode lasers as an excitation source was developed for chemical analysis of gas mixtures containing H<sub>2</sub>S, CO<sub>2</sub>, and CH<sub>4</sub>, allowing measuring both H<sub>2</sub>S at ppmv levels and CH<sub>4</sub> and CO<sub>2</sub> at up to 100% levels. Moreover, we compared these techniques in details in Table 1.

In this paper, we introduced a QEPAS sensor for simultaneous H<sub>2</sub>O, C<sub>2</sub>H<sub>2</sub>, and CH<sub>4</sub> concentration measurements by using three different QTFs with the resonant frequencies (f<sub>0</sub>) of 30.72 kHz, 32 kHz and 32.768 kHz in a small gas cell. Three distributed feedback (DFB) laser diodes operating at

1368.597 nm for H<sub>2</sub>O, 1653.722 nm for CH<sub>4</sub> and 1532.83 nm for C<sub>2</sub>H<sub>2</sub> were used as the excitation source. Finally, MDL of 1.3 ppmv, 79 ppmv and 5 ppmv have been achieved experimentally in the H<sub>2</sub>O, CH<sub>4</sub>, and C<sub>2</sub>H<sub>2</sub> with concentrations of 10000 ppmv, 85900 ppmv and 10000 ppmv, respectively. Preliminary measurements of the sensor response to H<sub>2</sub>O, C<sub>2</sub>H<sub>2</sub>, and CH<sub>4</sub> concentrations have been made with pure N<sub>2</sub> as a carrier gas, and the experimental results showed the relationship between second harmonic signal amplitude and the gas concentrations have a good linearity (H<sub>2</sub>O: R-square = 0.99979; CH<sub>4</sub>: R-square = 0.99881; C<sub>2</sub>H<sub>2</sub>: R-square = 0.99748). We also proposed a multi-QTFs theoretical model and verified that different frequency QTFs can work simultaneously. If more QTFs can be collimated, it is possible to detect more than three gases simultaneously.

## 2. Theory Analysis

### 2.1 Multi-QTFs Theory

According to the Beer-Lambert law, when a probe laser passes through a gas medium and is absorbed by gas molecules, the transmitted laser power can be expressed by Eq. (1):

$$I(v(t)) = I_i(v(t)) \cdot \exp[-S_i(T) g_i(v(t), v_0) PCL] \quad (1)$$

$I_i(v(t))$  stands for the incident laser power of each laser and  $I(v(t))$  for the transmitted laser power. Where  $S_i(T)$  is absorption line intensity of the different gas,  $g_i(v(t), v_0)$  is the linear function of gas absorption spectra,  $v(t)$  is the optical frequency,  $v_0$  is the frequency of spectral center, P is the gas cell pressure, C is the concentration of absorbing gas, L is the absorption path-length. When the output power of the laser is modulated periodically, the output laser power changes with time can be expressed as Eq. (2):

$$I_i(t) = I_i(v(t)) = I_c(t) + \Delta I \cos(\omega_i t - \Delta\varphi) i = 1, 2, 3... \quad (2)$$

Where  $I_c(t)$  is the laser power of the corresponding modulation center frequency,  $\Delta I$  is the intensity modulation amplitude,  $\omega_i$  is the modulation angle frequency,  $\omega_i = 2\pi f_i$ ,  $f_i$  is the modulation frequency (half of the resonant frequency of the different QTF in gas detection system),  $\Delta\varphi$  is the phase difference between the laser output power and the optical frequency.

In multi-QTF QEPAS system, the electrical signals detected by the detection circuit can be expressed as:

$$\begin{aligned} V_1(t) &= I_0(t) S_1(T) g_1(v(t), v_0) PCL \quad j = 1 \\ V_i(t) &= \prod_{i=2}^j \alpha_i \cdot [I_0(t) S_i(T) g_i(v(t), v_0) PCL] \quad j > 1 \end{aligned} \quad (3)$$

j is the order of the QTF.  $\alpha_i$  is the transmission rate when the laser passes through QTF<sub>i-1</sub>.

At room temperature and pressure, the absorption line is selected by Lorentzian curve, and Fourier expansion was made for  $g_n(v(t), v_0)$ :

$$g_i(v(t), v_0) = \sum_{n=0}^{\infty} g_{in}(x, m) \cos(n\omega_i t) \quad (4)$$

$g_{in}(x, m)$  is the Fourier expansion coefficient, x is the normalized frequency, m is the optical frequency modulation factor.

According to eq. (2), (3) and (4), the harmonic signal can be expressed as:

$$\begin{aligned} V_1(t) &= [I_c(t) + \Delta I \cos(\omega_1 t - \Delta\varphi)] \left[ \sum_{n=0}^{\infty} g_{1n}(x, m) \cos(n\omega_1 t) S_1(T) PCL \right] \quad j = 1 \\ V_i(t) &= [I_c(t) + \Delta I \cos(\omega_i t - \Delta\varphi)] \prod_{i=2}^j \alpha_i \left[ \sum_{n=0}^{\infty} g_{in}(x, m) \cos(n\omega_i t) S_i(T) PCL \right] \quad j > 1 \end{aligned} \quad (5)$$

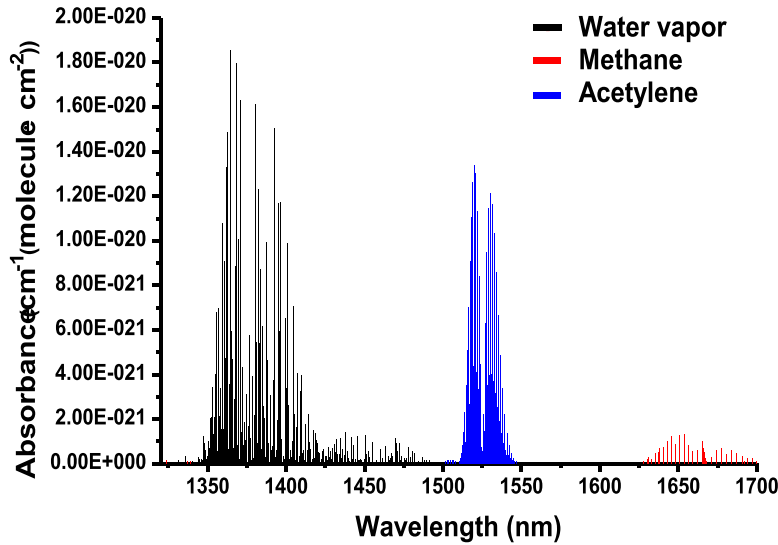


Fig. 1.  $\text{H}_2\text{O}$ ,  $\text{CH}_4$ , and  $\text{C}_2\text{H}_2$  absorption lines in the range of 1300 nm–1700 nm.

So the second harmonic signals of the different QTFs can be expressed as:

$$\begin{aligned}
 V_1(t) &= I_c(t)g_{12}(x, m)\cos(2\omega_1 t)S_1(T)PCL + \frac{1}{2}\Delta I g_{11}(x, m)\cos(2\omega_1 t - \Delta\varphi)S_1(T)PCL \\
 &\quad + \frac{1}{2}\Delta I g_{13}(x, m)\cos(2\omega_1 t + \Delta\varphi)S_1(T)PCL \\
 V_2(t) &= \alpha_2 I_c(t)g_{22}(x, m)\cos(2\omega_2 t)S_2(T)PCL + \alpha_2 \frac{1}{2}\Delta I g_{21}(x, m)\cos(2\omega_2 t - \Delta\varphi)S_2(T)PCL \\
 &\quad + \alpha_2 \frac{1}{2}\Delta I g_{23}(x, m)\cos(2\omega_2 t + \Delta\varphi)S_2(T)PCL \\
 V_3(t) &= \alpha_2 \alpha_3 I_c(t)g_{32}(x, m)\cos(2\omega_3 t)S_3(T)PCL + \alpha_2 \alpha_3 \frac{1}{2}\Delta I g_{31}(x, m)\cos(2\omega_3 t - \Delta\varphi)S_3(T)PCL \\
 &\quad + \alpha_2 \alpha_3 \frac{1}{2}\Delta I g_{33}(x, m)\cos(2\omega_3 t + \Delta\varphi)S_3(T)PCL \\
 &\dots \\
 V_j(t) &= \prod_{i=2}^j \alpha_i [I_c(t)g_{i2}(x, m)\cos(2\omega_i t)S_i(T)PCL] + \prod_{i=2}^j \alpha_i \left[ \frac{1}{2}\Delta I g_{i1}(x, m)\cos(2\omega_i t - \Delta\varphi)S_i(T)PCL \right] \\
 &\quad + \prod_{i=2}^j \alpha_i \left[ \frac{1}{2}\Delta I g_{i3}(x, m)\cos(2\omega_i t + \Delta\varphi)S_i(T)PCL \right]
 \end{aligned} \tag{6}$$

## 2.2 Selection of Gas Absorption Lines

Most of the current gas sensors use near-infrared laser as a light source for gas detection due to the matured semiconductor laser technologies [7], [21], [22], [23]. Fig. 1 depicts the  $\text{H}_2\text{O}$ ,  $\text{CH}_4$ , and  $\text{C}_2\text{H}_2$  absorption lines in the range of 1300 nm–1700 nm according to the HITRAN database [24]. Taking into account the cost and avoiding potential spectral interference between the three gases, three stronger absorption lines operating at 1368.597 nm for  $\text{H}_2\text{O}$ , 1653.722 nm for  $\text{CH}_4$  and 1532.83 nm for  $\text{C}_2\text{H}_2$  are selected. The intensities of their absorption lines are  $1.8 \times 10^{-20} \text{ cm}^{-1}(\text{molecule.cm}^{-2})$ ,  $1.32 \times 10^{-21} \text{ cm}^{-1}(\text{molecule.cm}^{-2})$  and  $1.035 \times 10^{-20} \text{ cm}^{-1}(\text{molecule.cm}^{-2})$ , respectively.

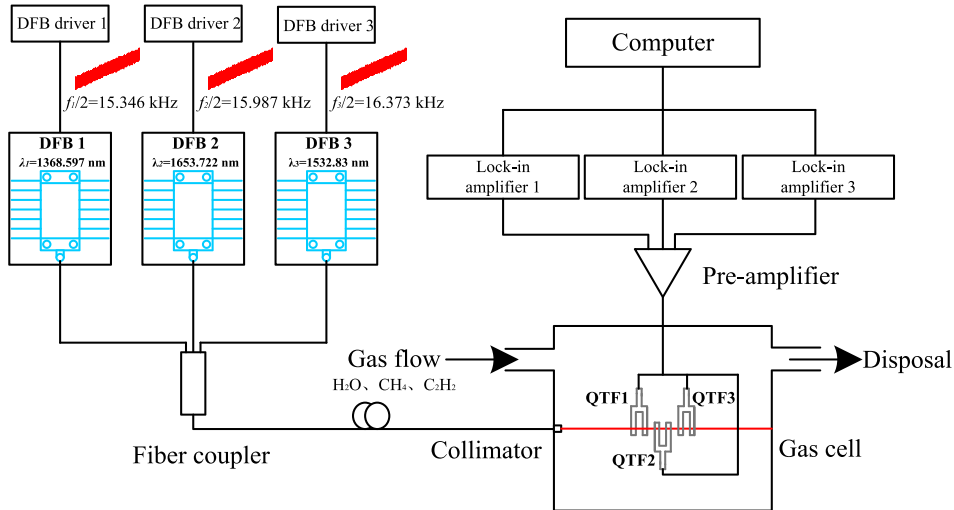


Fig. 2 Configuration of the multi-gas QEPAS sensor based on three different QTFs.

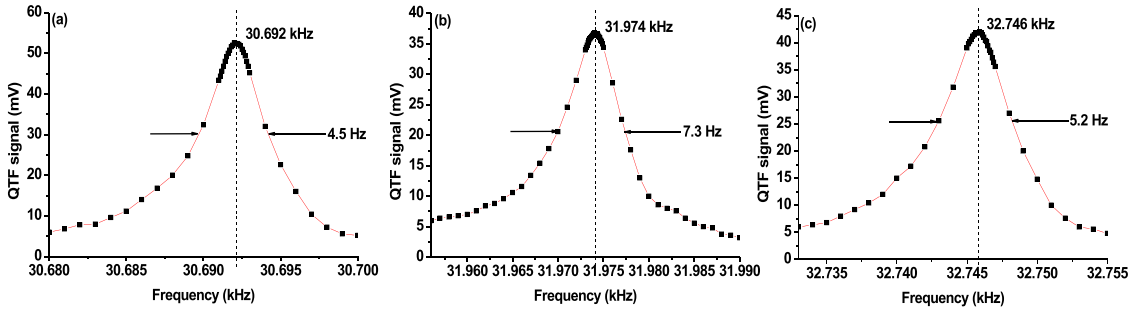


Fig. 3. Frequency response curve of different QTF. (a) QTF1, (b) QTF2, (c) QTF3.

### 3. System Configuration

A schematic of the experimental setup for multi-gas QEPAS sensor is shown in Fig. 2. Three 14-pin butterfly packaged DFB lasers with different central wavelengths were utilized as the light source. The DFB laser is controlled by a home-made drive circuit consisting of an ARM7 (LPC1758, NXP, Netherlands), a function generator (FY2300A, Feel Tech, China) and an adder, ARM7 is used to generate the sawtooth wave signal, the signal generator is used to generate the modulation signal (The modulation frequency is determined by the response frequency of the QTF). The adder adds the two signals as a laser drive signal. In order to prevent frequency interference, we chose three commercial QTFs (the gap between two prongs is  $\sim 300$   $\mu\text{m}$ ) with non-overlapping frequencies as the photoacoustic transducers. Their frequency response curves in the atmosphere are shown in Fig. 3. The Q-factor is defined as  $f_0 / \Delta f$ , where  $\Delta f$  represents the full width at half maximum (FWHM) of the resonance curve. The Q-factor of the three QTFs are about 6800, 4400 and 6300, respectively.

Fiber coupler was used as a beam combination. The laser beam propagates a gas cell with a G-lens fiber collimator. The laser beam passed through the three QTFs in order. To avoid background noise signal with a shifting fringe-like interference pattern shape, the focused laser should touch the tuning fork arms as little as possible. In this paper, three QTFs with different response frequency were used and mounted parallel pointing in opposite directions for a convenient spatial arrangement and the distance between the two QTFs is about 1.4 mm, as shown in Fig. 2. The current signal generated by the QTF is converted to a voltage signal by the pre-amplifier circuit. AD630 based

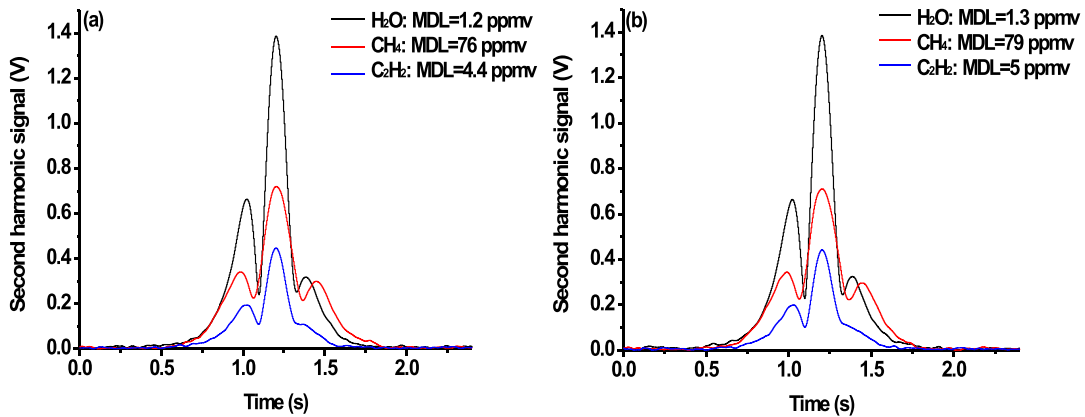


Fig. 4. Experimental second harmonic signal of H<sub>2</sub>O, CH<sub>4</sub> and C<sub>2</sub>H<sub>2</sub>. (a) Separate measurements of each gas. (b) Simultaneous measurement of three gases.

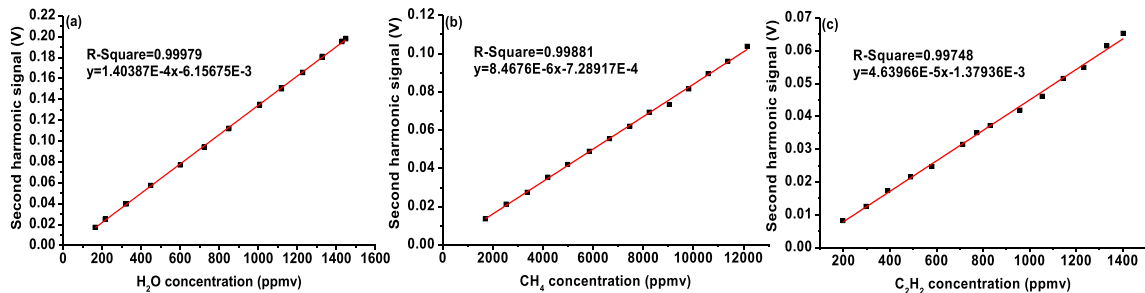


Fig. 5. Second harmonic signal as a function of gas concentration, the data points were the average value in different gas concentration repetitively recorded, at the pressure of 1 bar and temperature of 296 K. (a) Linearity of H<sub>2</sub>O. (b) Linearity of CH<sub>4</sub>. (c) Linearity of C<sub>2</sub>H<sub>2</sub>.

lock-in amplifier circuits are used to extract the harmonic signals. The computer is used to acquire the second harmonic signals.

#### 4. Experiment Results

The sensor system was evaluated for individual H<sub>2</sub>O, CH<sub>4</sub>, and C<sub>2</sub>H<sub>2</sub> detection and simultaneous H<sub>2</sub>O, CH<sub>4</sub>, and C<sub>2</sub>H<sub>2</sub> detection, respectively. The H<sub>2</sub>O, CH<sub>4</sub>, and C<sub>2</sub>H<sub>2</sub> with concentrations of 10000 ppmv, 85900 ppmv and 10000 ppmv were respectively injected into the gas cell. The second harmonic signal are shown in Fig. 4(a). The sensor noise was determined as a standard deviation from the signal far from the targeted absorption line. The signals and noise levels of each gas separately measured were about 1.39 V, 0.72 V, 0.45 V and 0.17 mV, 0.64 mV, 0.20 mV for H<sub>2</sub>O, CH<sub>4</sub>, and C<sub>2</sub>H<sub>2</sub>, respectively. The corresponding MDL were about 1.2 ppmv, 76 ppmv and 4.4 ppmv. Fig. 4(b). Shows the second harmonic signal obtained by injecting the mixture of three gases into the gas cell simultaneously. The signals and noise levels of three gases simultaneously measured were about 1.39 V, 0.71 V, 0.44 V and 0.18 mV, 0.65 mV, 0.22 mV for H<sub>2</sub>O, CH<sub>4</sub>, and C<sub>2</sub>H<sub>2</sub>, respectively. The corresponding MDL were about 1.3 ppmv, 79 ppmv and 5 ppmv. By comparing the MDL, the values measurement in the simultaneous are slightly higher than the ones measured for each single gas samples.

The linearities of the multi-gas sensor were evaluated by measuring its response to the different H<sub>2</sub>O, CH<sub>4</sub>, and C<sub>2</sub>H<sub>2</sub> concentrations. The results are shown in Fig. 5. All the measurements were performed at the pressure of 1 bar and temperature of 296 K. Several water vapor samples in different concentrations from 200 ppmv to 1400 ppmv were generated by a home-made

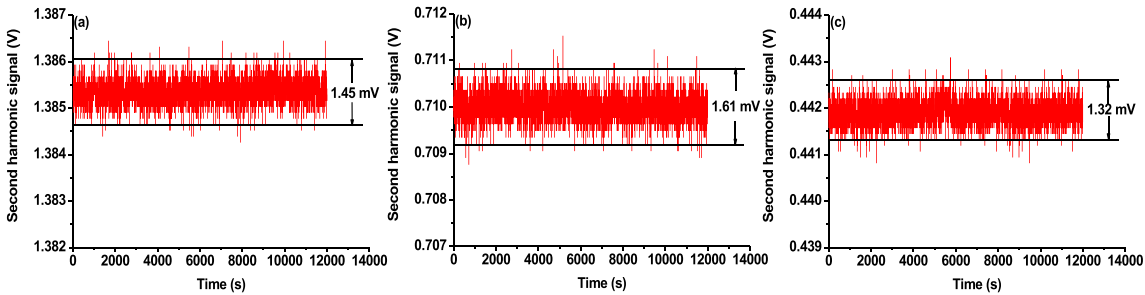


Fig. 6. Measurement results of simultaneous three gas concentrations monitoring for a 3.3 hour time duration, at the pressure of 1 bar and temperature of 296 K. (a) 10000 ppmv for  $\text{H}_2\text{O}$ . (b) 85900 ppmv for  $\text{CH}_4$ . (c) 10000 ppmv for  $\text{C}_2\text{H}_2$ .

dew-point generator. Several  $\text{CH}_4$  and  $\text{C}_2\text{H}_2$  samples in different concentrations from 1500 ppmv to 12500 ppmv and 200 ppmv to 1400 ppmv were generated by the gas mix system (RCS 2000-A, Beijing Kingsun Electronics, Beijing, China). A linear dependence of the second harmonic signal amplitude with the different gas concentrations is observed. The fitting curve Fig. 5. indicates a linear relationship ( $\text{H}_2\text{O}$ : R-square = 0.99979;  $\text{CH}_4$ : R-square = 0.99881;  $\text{C}_2\text{H}_2$ : R-square = 0.99748) in second harmonic signal amplitudes and gas concentrations, illustrating an excellent linear response of the multi-gas QEPAS sensor.

Finally, to evaluate the long-term stability of the multi-gas QEPAS sensor, the sensor system was used to simultaneously measure the second harmonic signal amplitude of  $\text{H}_2\text{O}$ ,  $\text{CH}_4$ , and  $\text{C}_2\text{H}_2$  at the certain concentrations. Measured second harmonic signal amplitude changes of  $\text{H}_2\text{O}$ ,  $\text{CH}_4$ , and  $\text{C}_2\text{H}_2$  over 3.3 hours are displayed in Fig. 6. It is observed that the second harmonic signal amplitude of  $\text{H}_2\text{O}$ ,  $\text{CH}_4$ , and  $\text{C}_2\text{H}_2$  were relatively stable during this period of time. All these measurements indicate that this multi-gas QEPAS sensor is capable of the simultaneous detection of  $\text{H}_2\text{O}$ ,  $\text{CH}_4$ , and  $\text{C}_2\text{H}_2$  with high stability.

## 5. Discussion

Such a sensor configuration has the advantage of significantly reducing the cost and simplifying the sensor system, and we can monitor more gases at the same time by increasing the number of QTFs. But the alignment of the QTFs is very difficult. The fiber coupler brings laser loss, which will cause the second harmonic signal amplitude to decrease, so improvement of this sensor MDL is an important issue and has to be considered for further developments in the future. This can be certainly achieved in a near future using higher power laser. And this technique can be readily employed to detect more gas species by properly choosing the DFB laser with different central wavelengths.

## 6. Conclusion

In conclusion, a multi-gas QEPAS sensor based on three QTFs has been demonstrated.  $\text{H}_2\text{O}$ ,  $\text{CH}_4$ , and  $\text{C}_2\text{H}_2$  were selected as the target analytes. Trace gas measurements of  $\text{H}_2\text{O}$ ,  $\text{CH}_4$ , and  $\text{C}_2\text{H}_2$  have been achieved with MDL of 1.3 ppmv at 1368.597 nm, 79 ppmv at 1653.722 nm and 5 ppmv at 1532.83 nm, respectively. And a good linearity was achieved. ( $\text{H}_2\text{O}$ : R-square = 0.99979;  $\text{CH}_4$ : R-square = 0.99881;  $\text{C}_2\text{H}_2$ : R-square = 0.99748). To demonstrate reliable and robust operation of the multi-gas QEPAS sensor a continuous monitoring of  $\text{H}_2\text{O}$ ,  $\text{CH}_4$  and  $\text{C}_2\text{H}_2$  concentration levels for a period of 3.3 hours were performed. Hence, the multi-gas QEPAS sensor is suitable for applications in environmental monitoring, industrial chemical analysis, atmospheric chemistry and biomedical and medical diagnostics as well as in law enforcement.

## References

- [1] D. D. Nelson, M. S. Zahniser, J. B. McManus, C. E. Kolb, and J. L. Jimenez, "A tunable diode laser system for the remote sensing of on-road vehicle emissions," *Appl. Phys. B-Lasers Opt.*, vol. 67, no. 4, pp. 433–441, 1998.
- [2] M. W. Sigrist, "Trace gas monitoring by laser photoacoustic spectroscopy and related techniques (plenary)," *Rev. Scientific Instrum.*, vol. 74, no. 12, pp. 486–490, 2003.
- [3] G. Durry, "Balloon-borne near-infrared diode laser spectroscopy for in situ measurements of atmospheric CH<sub>4</sub> and H<sub>2</sub>O," *Spectrochimica Acta Part A: Mol. Biomolecular Spectrosc.*, vol. 57, no. 9, pp. 1855–1863, 2001.
- [4] Y. Cao *et al.*, "Simultaneous atmospheric nitrous oxide, methane and water vapor detection with a single continuous wave quantum cascade laser," *Opt. Exp.*, vol. 23, no. 3, pp. 2121–2132, 2015.
- [5] J. P. Besson, S. Schilt, and L. Thevenaz, "Multi-gas sensing based on photoacoustic spectroscopy using tunable laser diodes," *Spectrochimica Acta Part A: Mol. Biomolecular Spectrosc.*, vol. 60, no. 14, pp. 3449–3456, 2004.
- [6] Q. Zhang, J. Chang, Q. Wang, Z. Wang, F. Wang, and Z. Qin, "Acousto-optic Q-switched fiber laser-based intra-cavity photoacoustic spectroscopy for trace gas detection," *Sensors*, vol. 18, no. 421, 2018.
- [7] A. Elia, P. M. Lugara, C. Di Franco, and V. Spagnolo, "Photoacoustic techniques for trace gas sensing based on semiconductor laser sources," *Sensors*, vol. 9, no. 12, pp. 9616–9628, 2009.
- [8] A. A. Kosterev, Y. A. Bakhirkin, R. F. Curl, and F. K. Tittel, "Quartz-enhanced photoacoustic spectroscopy," *Opt. Lett.*, vol. 27, no. 21, pp. 1902–1904, 2002.
- [9] P. Patimisco, G. Scamarcio, F.K. Tittel, and V. Spagnolo, "Quartz-enhanced photoacoustic spectroscopy: A review," *Sensors*, vol. 14, no. 4, pp. 6165–6206, 2014.
- [10] L. Dong, V. Spagnolo, R. Lewicki, and F. K. Tittel, "Ppb-level detection of nitric oxide using an external cavity quantum cascade laser based QEPAS sensor," *Opt. Exp.*, vol. 19, no. 24, pp. 24037–24045, 2011.
- [11] J. C. Petersen, L. Lamard, Y. Feng, J. F. Focant, and M. Lassen, "Quartz-enhanced photoacoustic spectroscopy as a platform for non-invasive trace gas analyser targeting breath analysis," 2017, arXiv:1704.07442.
- [12] C. Shi *et al.*, "A mid-infrared fiber-coupled QEPAS nitric oxide sensor for real-time engine exhaust monitoring," *IEEE Sensors J.*, vol. 17, no. 22, pp. 7418–7424, 2017.
- [13] Y. Ma, Y. He, Y. Tong, X. Yu, and F. K. Tittel, "Ppb-level detection of ammonia based on QEPAS using a power amplified laser and a low resonance frequency quartz tuning fork," *Opt. Exp.*, vol. 25, no. 23, pp. 29356–29364, 2017.
- [14] Y. Ma *et al.*, "Multi-quartz-enhanced photoacoustic spectroscopy," *Appl. Phys. Lett.*, vol. 107, 2015, Art. no. 0211062.
- [15] H. Zheng *et al.*, "Multi-quartz enhanced photoacoustic spectroscopy with different acoustic microresonator configurations," *J. Spectrosc.*, vol. 2015, 2015, Art. no. 218413.
- [16] P. Patimisco, A. Sampaolo, L. Dong, F. K. Tittel, and V. Spagnolo, "Recent advances in quartz enhanced photoacoustic sensing," *Appl. Phys. Rev.*, vol. 5, 2018, Art. no. 0111061.
- [17] W. Ren, W. Jiang, and F.K. Tittel, "Single-QCL-based absorption sensor for simultaneous trace-gas detection of CH<sub>4</sub> and N<sub>2</sub>O," *Appl. Phys. B-Lasers Opt.*, vol. 117, no. 1, pp. 245–251, 2014.
- [18] J. P. Besson, S. Schilt, and L. Thevenaz, "Multi-gas sensing based on photoacoustic spectroscopy using tunable laser diodes," *Spectrochimica Acta Part A: Mol. Biomolecular Spectrosc.*, vol. 60, no. 14, pp. 3449–3456, 2004.
- [19] H. Wu *et al.*, "Simultaneous dual-gas QEPAS detection based on a fundamental and overtone combined vibration of quartz tuning fork," *Appl. Phys. Lett.*, vol. 110, 2017, Art. no. 12110412.
- [20] A. A. Kosterev, L. Dong, D. Thomazy, F. K. Tittel, and S. Overby, "QEPAS for chemical analysis of multi-component gas mixtures," *Appl. Phys. B-Lasers Opt.*, vol. 101, no. 3, pp. 649–659, 2010.
- [21] Z.L. Wang, C.W. Tian, Q. Liu, J. Chang, Q.D. Zhang, and C.G. Zhu, "Wavelength modulation technique-based photoacoustic spectroscopy for multipoint gas sensing," *Appl. Opt.*, vol. 57, no. 11, pp. 2909–2914, 2018.
- [22] U. Troppenz *et al.*, "40 Gb/s directly modulated InGaAsP passive feedback DFB laser," in *Proc. 32nd Eur. Conf. Opt. Commun.*, 2006, pp. 61–62.
- [23] P. Werle, "A review of recent advances in semiconductor laser based gas monitors," *Spectrochimica Acta Part A: Mol. Biomolecular Spectrosc.*, vol. 54, no. 2, pp. 197–236, 1998.
- [24] L. S. Rothman *et al.*, "The HITRAN2012 molecular spectroscopic database," *J. Quantitative Spectrosc. Radiative Transfer*, vol. 130, pp. 4–50, 2013.